



## Analysis of pseudopathologies in *Edmontosaurus annectens* bones: taphonomic implications from biogenetic and diagenetic bone alterations from a Cretaceous bonebed in the Lance Formation, Wyoming

Bethania C. T. Siviero, Elizabeth Rega, Kevin E. Nick & Art V. Chadwick

**To cite this article:** Bethania C. T. Siviero, Elizabeth Rega, Kevin E. Nick & Art V. Chadwick (16 Jan 2026): Analysis of pseudopathologies in *Edmontosaurus annectens* bones: taphonomic implications from biogenetic and diagenetic bone alterations from a Cretaceous bonebed in the Lance Formation, Wyoming, *Journal of Vertebrate Paleontology*, DOI: [10.1080/02724634.2025.2600392](https://doi.org/10.1080/02724634.2025.2600392)

**To link to this article:** <https://doi.org/10.1080/02724634.2025.2600392>



© 2026 Bethania C. T. Siviero, Elizabeth Rega, Kevin E. Nick, And Art V. Chadwick.



[View supplementary material](#)



Published online: 16 Jan 2026.



[Submit your article to this journal](#)



[View related articles](#)



[View Crossmark data](#)



## ARTICLE

# ANALYSIS OF PSEUDOPATHOLOGIES IN *EDMONTOSAURUS ANNECTENS* BONES: TAPHONOMIC IMPLICATIONS FROM BIOGENETIC AND DIAGENETIC BONE ALTERATIONS FROM A CRETACEOUS BONEBED IN THE LANCE FORMATION, WYOMING

BETHANIA C. T. SIVIERO, <sup>1</sup> ID \*<sup>1</sup> ELIZABETH REGA, <sup>2</sup> ID <sup>2</sup> KEVIN E. NICK, <sup>3</sup> ID <sup>3</sup> and ART V. CHADWICK <sup>4</sup> ID <sup>4</sup>

<sup>1</sup>Department of Pathology and Human Anatomy, Loma Linda University, Loma Linda, California 92350, U.S.A., bsiviero@llu.edu;

<sup>2</sup>Department of Medical Anatomical Sciences, Western University of Health Sciences, Pomona, California 91766, U.S.A., erega@westernu.edu;

<sup>3</sup>Department of Earth and Biological Sciences, Loma Linda University, Loma Linda, California 92350, U.S.A., knick@llu.edu;

<sup>4</sup>Department of Biology, Southwestern Adventist University, Keene, Texas 76059, U.S.A., chadwick@swau.edu

**ABSTRACT**—Pseudopathology in paleontology refers to postmortem bone alteration mimicking osseous features of disease. Differentiating pathologies from pseudopathologies is critical in the investigation of paleopathology, as misattribution can produce erroneous conclusions regarding diseases and life history. In this paper, we describe several examples of pseudopathologies from a Cretaceous commingled monospecific bonebed of *Edmontosaurus annectens* (Lance Formation, WY). In addition to 96 documented real pathologies or injuries uncovered in examination of over 3000 fossil bone specimens, multiple pseudopathologies were observed. Most of these were bone fractures or patterned erosions of bone material resulting from most likely taphonomic processes. Bone proliferation characterizing the living response to premortem injuries is one clue. Absent this response, perimortem injuries and postmortem changes due to scavenging, weathering, and other factors should be considered. CT imaging of one astragalus showed intense focal radiodensity surrounding the two large lesions, sharply distinct from the surrounding bone. When compared against histological thin sections and SEM-EDS scanning, what appeared in CT as dense sclerotic reactive bone suggested postmortem migration of minerals subsequent to erosive insect boring, a gradient potentially related to the unique microenvironment thereby created affecting subsequent permineralization. Evidence from our analysis of this assemblage supports that even diagnoses supported by non-invasive imaging such as CT scans should, when possible, be tested by histological analysis. Otherwise, a distinctly and disturbingly non-zero number of erroneous conclusions are to be expected from any survey of paleopathology, particularly given the numbers of intervening processes separating a fresh carcass from permineralized bone.

**SUPPLEMENTARY FILE(S)**—Supplementary file(s) are available for this article for free at [www.tandfonline.com/UJVP](http://www.tandfonline.com/UJVP)

Citation for this article: Siviero, B. C. T., Rega, E., Nick, K. E., & Chadwick, A. V. (2026) Analysis of pseudopathologies in *Edmontosaurus annectens* bones: taphonomic implications from biogenetic and diagenetic bone alterations from a Cretaceous bonebed in the Lance Formation, Wyoming. *Journal of Vertebrate Paleontology*. <https://doi.org/10.1080/02724634.2025.2600392>

Submitted: March 14, 2024

Revisions received: November 21, 2025

Accepted: November 24, 2025

## INTRODUCTION

Of the conspicuous and dramatic bone alterations in the fossil record attracting considerable comment, the alterations garnering the most attention are bite marks (tooth traces) and diseases, largely because of their potential to address individual and group

life history. Many infectious and traumatic pathologies are associated with evidence of bone remodeling indicating that the animal lived with the injury long enough for bone to respond. Tooth traces (with few exceptions) and unhealed fractures in contrast suggest peri- or postmortem bone alteration and are most challenging to diagnose. Due to postmortem and/or post-burial biogenetic and diagenetic taphonomic processes, imposed alterations to bone surfaces have the potential to mimic these perimortem bone lesions (Hacket, 1981; Rothschild et al., 2023). These types of postmortem bone modification are known as pseudopathologies and must be distinguished from true pathological bone abnormalities, since their misidentification can lead to erroneous conclusions about diseases and living conditions of animals represented in the fossil record.

Examples of pseudopathologies occur throughout the fossil record but are largely anecdotal in their reporting. Some pseudopathology descriptions are embedded in paleopathological analyses of isolated remains (Hanna, 2002; Odes et al., 2017; Scott et al., 2015), while others are reports focusing on different

\*Corresponding author.

© 2026 Bethania C. T. Siviero, Elizabeth Rega, Kevin E. Nick, And Art V. Chadwick.. This is an Open Access article distributed under the terms of the Creative Commons Attribution-NonCommercial-NoDerivatives License (<http://creativecommons.org/licenses/by-nc-nd/4.0/>), which permits non-commercial re-use, distribution, and reproduction in any medium, provided the original work is properly cited, and is not altered, transformed, or built upon in any way. The terms on which this article has been published allow the posting of the Accepted Manuscript in a repository by the author(s) or with their consent.

Color versions of one or more of the figures in the article can be found online at [www.tandfonline.com/UJVP](http://www.tandfonline.com/UJVP).

types of postmortem bone modifications from fossil assemblages with the goal of describing taphonomy or life history (Lopes & Ferigolo, 2015; Roberts et al., 2007). Boring insects are commonly proposed agents of erosive changes causing bone depression/erosions (Csiki, 2006; Hasiotis et al., 1999; Lima, 2017; Martin & West, 1995). Weathering by plant roots growing in contact with bone (root traces) can mimic the vascular depressions seen in inflammatory bone pathology (Halstead, 1990). Peri- and postmortem fractures often result from processes that can readily confuse the examiner into characterizing them as evidence of predation or trauma. Other agents besides invertebrate/vertebrate animal feeding are water and wind erosion, weathering, abrasion, and transport (Behrensmeyer, 1978; Blau, 2017; Conard et al., 2008; Egeland & Pickering, 2021; Littleton, 2000; Thompson et al., 2011). All are mechanisms that can alter bone morphology and texture in postmortem.

Pseudopathology results from biogenetic and diagenetic processes affecting both permineralized and unaltered fossil bone. In this way, pseudopathology is further defined in this paper as diagenetic and/or biogenetic bone modifications not attributable to premortem predation, trauma, or disease. Systematic observations of such pseudopathologies on bone have heretofore largely been the purview of those seeking to understand depositional environments of the fossils, where such traces are characterized as “taphonomic factors.” Routinely, in our work and that of others, pseudopathologies are the boring extras tucked away in the supplemental material adjacent to stimulating “paleo-diagnoses.” In any analysis of proper paleopathology, pseudopathology must be the first diagnosis to exclude and therefore deserves closer examination concerning its diagnostic criteria. Evidence from analysis of this assemblage supports that most diagnosis can be achieved by non-invasive procedures such as macroscopic observations and CT scans. In the case of more ambiguous bone alterations, microscopic analysis, when possible, can also be beneficial for diagnosis.

While most pseudopathologies manifest as areas affected by erosive changes or fracture, other modifications can occur that mimic pathology. These include bone shape deformations, caused from rapid burial during early postmortem stages while the bone is still fresh or “green” (Petersen et al., 1972) and other taphonomic processes, such as bioerosion and sediment abrasion, altering bone shape over time (Pokines & Higgs, 2021). In such cases, the resulting smooth bone deformation can easily be confused for a pathology, such as shaft angulation due to a healed fracture, the sequelae of a bone mineral density deficiency (such as osteomalacia/rickets) and other developmental/metabolic/idiopathic etiologies.

Other confusing mimics of pathologies arise from the normal and natural variation of anatomical bone features. Such variations are common between species and within bones from the same species, especially those of different developmental ages. Markings of vasculature and nerve foramina, although mostly consistent in location, can all too often be variable in shape and position, and caution must be exercised in interpreting these features absent comparative material, especially with features varying between species (Siviero, 2019). While it may seem obvious, the familiarity of the researcher with the natural bone morphology of the taxa being examined and with the different bone types amongst different species is imperative and can only be achieved after observing many specimens (Johnson et al., 2017; Kizilkanat et al., 2007; Seymour et al., 2024; Zoetis et al., 2003). This experience is critical especially given the clinical literature on pathology in extant animals is heavily biased toward mammals and may not remotely reflect the conditions of the taxon being examined in bone ontogeny or structure.

Fossil preparation is another important consideration in studying bone alterations such as pathologies or pseudopathologies (Siviero et al., 2017; Wiest et al., 2018). Mineral adhesion to

bone surfaces due to post-burial diagenetic processes sometimes appears to result from bone reactivity/proliferation, thus credibly mimicking manifestations of osteophytes or exostosis. The fossil preparator or examiner may be aware and able to distinguish the biogenetic bone from adhering matrix and/or bone fragments cemented onto the surface. However, the researcher must always be on the lookout for these “adhesions” particularly in bones with irregular surface cracking and other conspicuous accumulative alterations. On some occasions, only microscopic thin sections can truly distinguish adhered bone fragments and minerals from a proliferative lesion.

On the other hand, the fossil preparator must also be careful not to overly prepare bone surfaces. Even if they appear unusual, bone surface textures must be preserved to not eliminate, erase, or shave the more superficial types of bone remodeling/reactivity or lesions suggestive of pathology.

A tooth trace in a fossil bone is a type of puncture, slice, or drag lesion acquired pre-, peri-, or postmortem from the dentition of a predator or scavenger. These lesions are more popularly termed “bite marks” in popular literature. Interest in this rare type of injury is high—most likely due to its potential usefulness in providing dramatic evidence for prehistoric behavior. However, the existence of tooth traces, although potentially camouflaged and underrepresented in the fossil record due to bone healing of those lucky enough to survive predation events, can also be exaggerated if the investigator confuses various pseudopathologies with true tooth traces.

The diagnostic criterion of bone response to injury is challenged by the perimortem nature of some vertebrate tooth traces on bones. Elsewhere, we have argued that evidence for the dental origin of features attributed to tooth traces is truly only diagnostic if associated with serrations and/or parallel striations corresponding to the inflictor’s tooth denticles and/or bite morphology (Siviero, 2019). Tooth trace-like pseudopathologies can be caused by postmortem puncture, insect boring (bioerosion) and fossil over-preparation. Punctures and pits with evidence of drag marks that reflect the bite infliction and the consequent movement while the predator is engaged are considered more conclusive of tooth traces, if clear denticle striation marks are lacking (Binford, 1981; Pobiner, 2008; Pobiner et al., 2007). Many depressions or holes mimic tooth traces. Bone neurovascular foramina, bone erosions from tumors, cysts, cartilaginous inclusions, infectious granulomas, and cloaca-like channels for pus drainage are some examples that can be mistaken for marks of teeth by their shape location and orientation (Siviero et al., 2020b; Wolff et al., 2009).

Although attempts to develop criteria for the distinction between pathology versus pseudopathology in animal skeletons have been proposed (Corron et al., 2017; Lima, 2017), ultimately, their usefulness cannot replace the multidisciplinary expertise of paleopathologists in providing diagnostic criteria. Current consensus is that evidence of bone reactivity in association with bone abnormality suggests pre-mortem injury and partial recovery, thus underscoring the nature of the genuine pathology (Corron et al., 2017; Lima, 2017; Rothschild et al., 2023; Scott et al., 2015; Siviero et al., 2020a).

The bones examined in this study are from a largely monospecific bonebed from the Upper Cretaceous Lance Formation in northeastern Wyoming containing mixed bones of adult *Edmontosaurus annectens*. The bones are well-preserved, mostly disarticulated, disassociated, and have no apparent spatial orientation indicative of flowing water current (Snyder et al., 2020; Weeks, 2016). In addition, taphonomic analysis of the bonebeds suggests an assemblage exposed for a short time after death (enough time to decompose, disarticulate, and dissociate), followed by a final burial resulting from a mass flow (Snyder et al., 2020; Weeks, 2016).

In addition to 96 documented pathologies or injuries uncovered in examination of over 3000 elements (Siviero, 2019), multiple pseudopathologies were observed in this assemblage, mostly postmortem bone fractures or patterned depressions resulting from erosion and/or insect damage mimicking various pathological lesions. In this study, we examine bone abnormalities from one of a series of massive *Edmontosaurus annectens* monospecific Cretaceous (Maastrichtian) bone beds in the Lance Formation, eastern Wyoming. Thereby, we (1) add to the descriptive literature of fossil bone pseudopathologies, (2) collect and analyze additional bone-specific data regarding site taphonomy, and (3) include a cautionary example that highlights the value of using different diagnostic methods, such as radiography and histological analysis (when possible), to accurately confirm a diagnosis—especially when lesions are more ambiguous.

## MATERIALS AND METHODS

In total 3013 individual specimens of whole bones and bone fragments from a monodominant *E. annectens* bonebed excavated at the Hanson Research Station (HRS), in northeastern Wyoming, and stored at the Southwestern Adventist University (SWAU) dinosaur museum in Keene, Texas were analyzed. The first author examined bone collected and prepared from 1997–2017 from the South and North quarries for bone pathologies as part of ongoing multi-year collaborative analysis. Ninety-six bones with conspicuous lesions resembling erosive and fracture/tooth trace marks were further examined. Initial screening for pathology relied on macroscopic examination, assisted by a 10 $\times$  lens magnifier, Dino-Lite microscope, and stereo microscope while in the collections. Because the initial collection of affected elements for further analysis was predicated on macroscopic morphological screening with subsequent microscopic reexamination, pathologies and pseudopathology contained entirely within the interior of the elements will have been inevitably missed during screening, a common weakness in analyses relying on macroscopic screening (Martin, 2008).

Of these bones with lesions identified by macroscopic examination, we selected several for further analysis, which we describe in this study. These elements were photographed, and two specimens further subjected to CT scans taken at the Radiology Department at Loma Linda Medical Center (LLMC) with a CT LightSpeed VCT model from GE medical system. Scan parameters were set for 400 kV (for HRS12255) and 500 kV (for HRS09967), amperage of 500 mA, pixel spacing of 0.5351 mm  $\times$  0.5351 mm and slice thickness of 1.3 mm. These images are available for viewing at MorphoSource <https://www.morphosource.org> (for specimen HRS12244 search as 12244; and for specimen HRS09967 search as 9967).

A further subset of two elements was prepared for histological examination at Loma Linda University (LLU), Department of Earth and Biological Science. Prior to bone sectioning for histological analysis, molds and casts of each specimen were prepared with Dragon Skin™ and Smooth-Cast® 300 from Smooth-On, Inc. (Macungie, PA). Subsequently, specimens were sectioned and polished for high-resolution scanning (Epson Perfection V600 Photo) and traditional thin sections were prepared at LLU utilizing standard techniques. Due to the difficulty in interpreting specimen HRS12244, it was prepared for scanning electron microscopy with energy-dispersive X-ray spectroscopy (SEM-EDS) for analysis at LLU. EDS detects elements in samples, allowing for mineral identification. The first and second authors evaluated the set of bones with observed surface manifestations for final differential diagnosis. Additional images of specimens reported in this study that lack figures in this paper are available for viewing in the SWAU fossil catalog available at <https://fossil.swau.edu>.

**Institutional Abbreviations**—**HRS**, Hanson Research Station, Roxson, WY, U.S.A.; **LLMC**, Loma Linda Medical Center, Loma Linda, CA, U.S.A.; **LLU**, Loma Linda University, Loma Linda, CA, U.S.A.; **SWAU**, Southwestern Adventist University, Keene, TX, U.S.A.

## RESULTS

From the 3013 specimens examined, 96 with macroscopically apparent defects were further analyzed. Eight specimens with modifications ultimately attributed to postmortem biogenetic or diagenetic modification often mimicking pathology were identified. These eight were specimens with sufficiently similar appearance to pathological bone lesions such genuine confusion could result, especially for the untrained eye. These specimens do not represent the exhaustive pool of all postmortem specimens displaying features readily attributable to taphonomic change. Abundant evidence of obvious environmental erosion on elements such as vertebrae were not included for analysis after initial examination and dismissal from consideration. It is the lesions of ambiguous generation that were the focus of our investigation, with an eye toward potentially eliminating specimens from the category of pseudopathology specimens actually showing reactive bone indicative of post-injury healing.

Descriptions in this Results section are restricted to specimens with conditions sufficiently resembling pathology as to be typically reported as pseudopathological. In the case of tooth traces, diagnostic criteria refer to those in the literature (Binford, 1981; Jacobsen & Bromley, 2009; Mikuláš et al., 2006; Njau & Blumenschine, 2006; Pobiner, 2008; Pobiner et al., 2007).

### A Note on Rib Fractures

We do not report in detail herein on peri- and postmortem bone fracture, a phenomenon commonly observed in these bonebeds. As expected, some ribs had collection or load fractures with crumbly surfaces on fractured sites. Several other ribs (mostly in complete specimens) also have their distal end missing but with angled and smooth surface texture on the fractured site (Fig. S1). These fractures frequently occur in the distal end of ribs, with a smooth fracture plane, indicating that the fracture occurred while the bone was still green suggesting early perimortem or postmortem fracture. Thus, some of these fractures can result from ribcage breakage during scavenging in the attempt to access the organs, although early postmortem transport can also account for some of the rib fractures. Their manifestations are important in paleopathological analysis, especially when attempting to understand taphonomic conditions associated with the animal remains. The etiologies associated with bone fractures with no evidence of bone remodeling, are more difficult to determine for they can result from different processes, including peri- or postmortem damage. It is important to determine the types and patterns of fracture since these can indicate breakage while the bone was still fresh/green or brittle and also if force was directly applied, resulting in breakage (Resnick, 1995; Rixford, 1913). Peri- or postmortem bone fractures can result from an attack, scavenging, transport, compaction, and excavation or collection damage. If the cause of a fracture is mistaken, the conclusions pertaining to the animal's conditions and associated taphonomic processes will be misinterpreted or exaggerated.

### Description of Linear and Circular Features Perforating the Cortex

**Rib Fragment HRS03161**—This specimen displays a cluster of finely curvilinear areas of bone bleaching from 0.5–1 mm in width and 1 cm or more in length, resembling clusters of tiny

worms (Fig. 1A). Also displayed on the surface of the bone is a puncture with a directly associated groove mark (Fig. 1A) and no bone reaction.

**Rib Fragment HRS02038**—A similar juxtaposition of processes is present on this rib fragment specimen (Fig. 1B, C). The fractured end shows irregular dull edges. The bone surfaces of the unfractured end of the rib manifest juxtacortical proliferation of bone. The surfaces also show modified texture by the deterioration of the cortical bone and partially exposing the medullary bone (Fig. 1B, C).

**Cervical Vertebra HRS10676**—Specimen has multiple subcircular depressions with diameters between 5–20 mm and depths of 1–7 mm. These lesions present no associated bone reaction or increase in density (Fig. 2A). The borders appear irregularly wavy and the surface area, deep into the lesion, is also irregularly perforating the cortical bone and exposing medullary bone. Several smaller pitted lesions are individual, but coalescing pitting is also displayed. Flaking and cracking of the bone surface is also shown.

**Metatarsal HRS12360**—Two areas of deep parallel scores or furrow-like linear grooves, mimicking erosive pathological lesion 1–2.5 mm in width, up to 3 mm in depth and up to 30 mm in length, were observed on the medial and lateral surface of a right metatarsal II (Fig. 2B, C). These structures present a dramatic appearance. They are parallel and evenly spaced on the distal and proximal end of the bones. Distally, five parallel scores are seen on the dorsal aspect (Fig. 2B), and two more on the plantar aspect (Fig. 2C). Proximally, the plantar side shows two more parallel grooves (Fig. 2C). These marks are even in depth, and no apparent bone reaction is associated with them. Other metatarsal bones within the collection (HRS05905, HRS15494) also present postmortem bone surface alterations with similar orientation and morphology.

**Distal Caudal Vertebra HRS14005**—This specimen bears two sets of overlapping features. The bone surface texture on the proximal and distal intervertebral articular surfaces manifests several associated tiny shallow regular depressions/pits, each less than 0.5 mm in diameter spread across both surfaces (Fig. 3). The depth of these tiny depressions is less than 0.5 mm, eroding into the cortex exposing the medullary bone.

On the caudal centrum surface, another set of features in the form of two large, shallow hemispherical pits is present. The dorsal lesion is ovoid, 10 mm × 5 mm. A similar, smaller angular teardrop depression 3 mm × 5 mm, 2 mm in depth is present near the ventral centrum margin. Both shallow hemispherical concavities have margins with the surface cortical bone that are sharp. Although both perforate into the spongy bone of the centrum, the cavities' depth and walls are smooth with no scallops. Additional caudal centra specimens within this bone collection manifest similar bone modifications (HRS02042, HRS02807, HRS02890, HRS09591).

**Ischium HRS12443**—This specimen manifests distinctive patches of cortical alteration on the external and internal surfaces (Fig. 4A). These alterations have the appearance of multiple coalescing foci of cortical delamination, with isolated and/or overlapping shallow circular-elliptical pits or depressions varying between 0.5 to 1 cm in length, 0.5 cm in width, and >1 mm in depth. The edges of the walls from several of these pits (especially noted in isolated examples) are scalloped and some have an unmodified pedestal in the center of the pit (Fig. 4B). Most of the floors of these shallow pits underscore the layered nature of the bone removal (Fig. 4B). The shallow pits are also associated with some flaking (Fig. 4B). Due to the specimen's rarity, it was not deemed necessary by the authors to section this.

**Astragalus HRS12244**—This specimen manifests two very prominent adjacent deep depressions in the distal dorsal surface, adjoining the metatarsal joint (Fig. 5, features 1 & 2). These

circular lesions are 0.6–1 cm in diameter at the cortical surface with smoothly sloping surface edges into the depths of the pit. Feature 2 has a distinct 3–5 mm sloping margin surrounding the pit. CT scan imaging and histological cross sections of bone found depressions with well-defined edges penetrating the cortical bone, approximately 0.8–1 cm in depth, with the surface opening width smaller than the erosion width inside the bone (Fig. 5B, C, D). The shape of the base of both lesions is evenly concave, lacking the pointed apex that could be expected in a perimortem tooth puncture of this depth. CT scan imaging shows a distinct focal brighter (more radio-opaque) area surrounding both depression sites, manifesting most strongly around feature 1 (Fig. 5B). Based on the CT images alone, the appearance is that of a reactive sclerotic bone surrounding a necrotic area. Thus, at first glance, it would appear these lesions were premortem osseous response. However, additional tests were to challenge this interpretation.

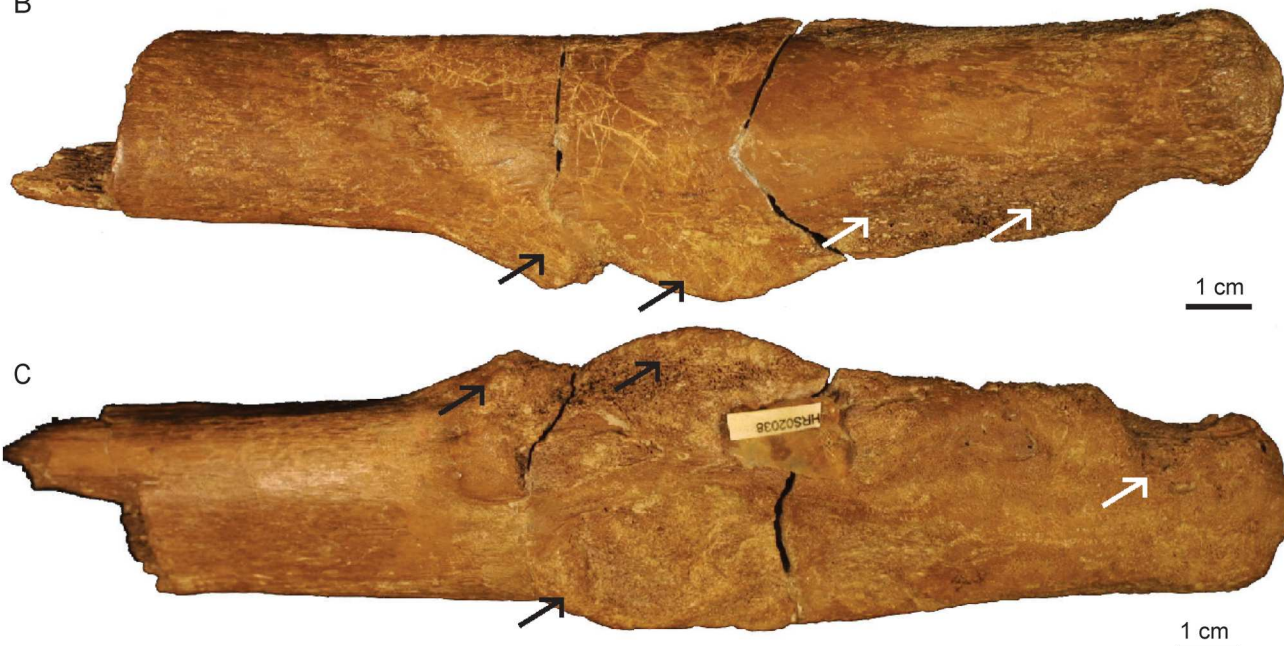
Histological images (thin sections) show sharply truncated fibrolamellar bone (FLB) consistent with other FLB descriptions (Chinsamy et al., 2012; Whitney et al., 2022). The lamellae are continuous with the underlying bone extension edge of depression 1 (Fig. 5E, F). The edge of the depression shows individual lamellae sharply terminating against the depression, with small fissures, creating a bumpy surface at the interface. No reactive new bone proliferation is present. Important features that could indicate the microtrauma of an unhealed large puncture, like that made by a tooth, such as displaced lamellae fragments or spalls on the lesion margin are also lacking. Furthermore, a thin dense adhering layer of matrix is clearly in evidence, occluding the sharp margins of the depression (Fig. 5E). This area of bone displayed a more intense red coloration surrounding and directly adjacent to the depression site (Fig. 5E); these redder areas in the thin section correspond to the brighter regions in the CT scan imaging. Microscopic examination in reflected light shows the presence of pyrite and hematite with greater concentration of hematite adjacent to the depression (Fig. S2). The pyrite crystals ( $FeS_2$ ) are present as irregular shaped microcrystalline aggregates and frambooids ranging from 10–20  $\mu m$ . Pigment-sized hematite crystals are distributed within the bone next to the lesion and cause the dark red coloration from local oxidation of pyrite. SEM-EDS analysis of a sectioned surface through the depression demonstrates the presence of sulfur and iron in the bone, with iron concentration decreasing away from the depression (Fig. S2). We observed a small amount of woven bone characteristic of new premortem bone deposition at the bone articular surface. This is expected because these surfaces are constantly remodeling in response to stress.

**Pedal Phalanx HRS09967**—Pedal phalanx III-2 manifests a series of pockmarked depressions on the proximal and distal articular surfaces (Fig. 6A, B). However, arrangement and morphologies of depressions between the two surfaces, have different depth and size distributions. Depressions on the proximal surface have irregular outline distributed on the bone surface with no particular arrangement, but all penetrate cancellous bone (Fig. 6A). Their outline is irregular with curved edges. Depth of the depressions range from 0.3–0.8 cm. CT scan shows no increase in bone density on the surfaces directly associated with depressions (Fig. 6C). Histological analysis of the area associated with depression shows the presence of organized bone tissue underlying localized bone destruction, but no bone deposition or remodeling directly associated with depression. Since the depression is associated with an articular surface some bone modification is noted, and expected, due to normal stress in the joint (Fig. 6D). On the distal articular surface, the depressions are also randomly distributed, have regular circular shapes, surface diameters ranging from 1–3 mm, and depths of 1 mm that do not penetrate into cancellous bone. No change in bone density was shown in CT images (Fig. 6C). On the left

A



B



C

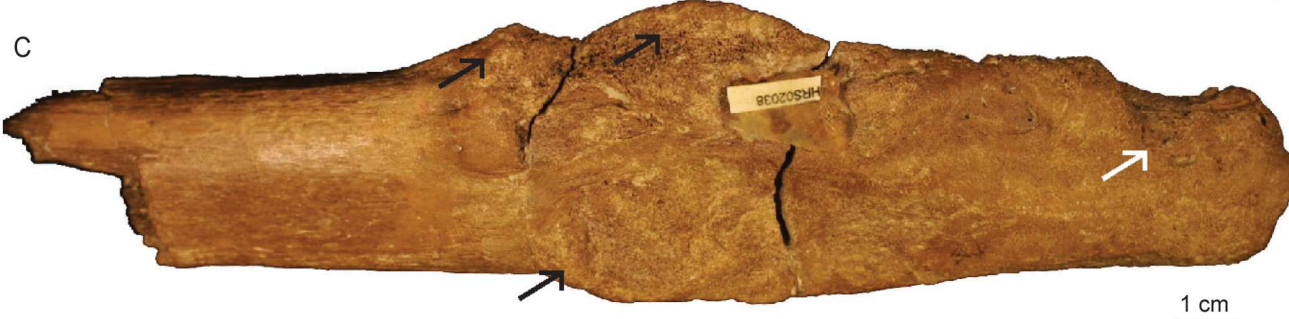


FIGURE 1. Fossil rib fragments from *Edmontosaurus annectens* with modifications. **A**, rib fragment HRS03161 with root traces (indicated by white arrow) and tooth trace (indicated by black arrow); **B**, view of the inner surface of the distal end of rib fragment HRS02038 with neoplasm and pseudopathology; **C**, view of the outer surface of the distal end of rib fragment HRS02038. Black arrows point to evidence of bone proliferation suggestive of neoplasm in **B** and **C**. White arrows point to postmortem textural changes on bone surfaces in **B** and **C**.

edge of the same bone surface, a depression resembling those on the proximal surface (Fig. 6D) is observed, similar to the one located on the superior edge of the proximal surface of the bone (Fig. 6A). Abrasion on both articular surfaces is also observed but it is more evident on the proximal surface of the bone.

## DISCUSSION

A summary table of our findings with descriptions and associated diagnosis can be found in the supplementary material (Table S1). First, it is critical to underscore the importance of differentiating real from pseudo pathological lesions. Both real pathology and other surface modifications, causing lesions on bone surfaces, are present on two rib fragments (Fig. 1). Rib fragment HRS03161 shows the presence of clusters of finely curvilinear areas of bone bleaching. These clusters are both common in this assemblage and morphologically rather characteristic for root traces (Behrensmeyer, 1978; Schultz & Dupras, 2021).

Manifestations of root traces were commonly found in specimens from this bonebed collection. Root traces are thought to be the result of diagenetic changes in the bone material adjacent to ingrowing roots. Selective mineral movement (leaching) from the fossil into surrounding plant roots or in the reverse may be the cause of the color change (Behrensmeyer, 1978; Schultz & Dupras, 2021). Determination of the precise mechanism of the color change is a subject for future inquiry. The puncture and groove displayed on the same bone surface, is identified as a tooth trace further diagnosed by the presence of a drag mark (Fig. 1A). Thus, HRS03161 displays both the characteristic pseudopathological root trace and a genuine tooth trace. That the bone damage in the latter was acquired peri- or postmortem is evident, due to the absence of bone reaction. The bonebed does contain multiple examples of lesions (examined elsewhere) attributable to the marks of teeth during predation or scavenging on diagnostic grounds from the literature (Siviero et al., 2020a).

Rib Fragment HRS02038 (Fig. 1B, C) shows a fractured end with irregular edges suggestive of a postmortem fracture

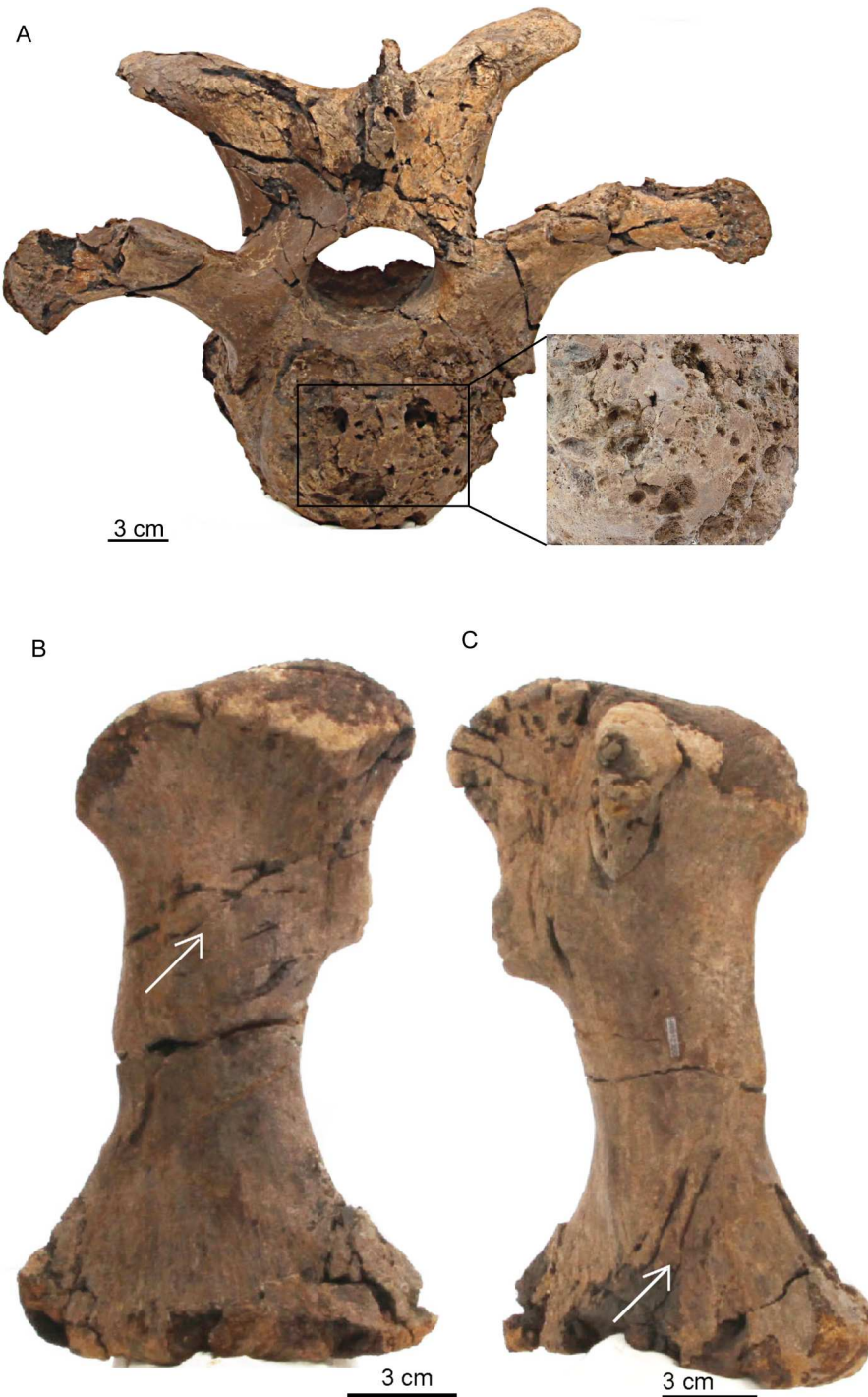


FIGURE 2. Fossil bones from *Edmontosaurus annectens* with pseudopathologies. **A**, cervical vertebra HRS10676 with postmortem depressions created by surface exposure, including a closer view of the surface in a different angle for better view; **B** and **C**, medial and lateral views of right metatarsal II HRS12360 with parallel linear marks indicated by the arrows.

(Mann & Hunt, 2013). The bone also has prominent areas of subperiosteal bone proliferation on the internal and external distal surfaces strongly resembling the pattern encountered in cases of periosteal elevation associated with trauma and infection (Landry et al., 2000; Whiteside & Lesker, 1978). The ribs are a frequent location of subperiosteal proliferation, due to their superficial subcutaneous position and the function and mechanical insults they endure. This is the sole example in this paper of a specimen manifesting new bone proliferation (Fig. 1B, C). The nature of this abnormality and location suggests a bone

reaction to a musculocutaneous lesion, a true pathology. The same surface also shows texture modification with the appearance of “fine pitting” suggesting cortical bone deterioration. Cortical bone porosity in pre-mortem specimens suggests pathology such as osteoporosis (Lin & Lane, 2004; Seeman, 2013), porotic hyperostosis (Holland and O’Brien, 1997; Stuart-Macadam, 1991), and osteodystrophy (Sharma et al., 2018). However, in fossil bones, cortical bone porosity can also indicate taphonomic processes that cause the delamination of cortical bone due to bone exposure, such as in the cause of subaerial bone surface

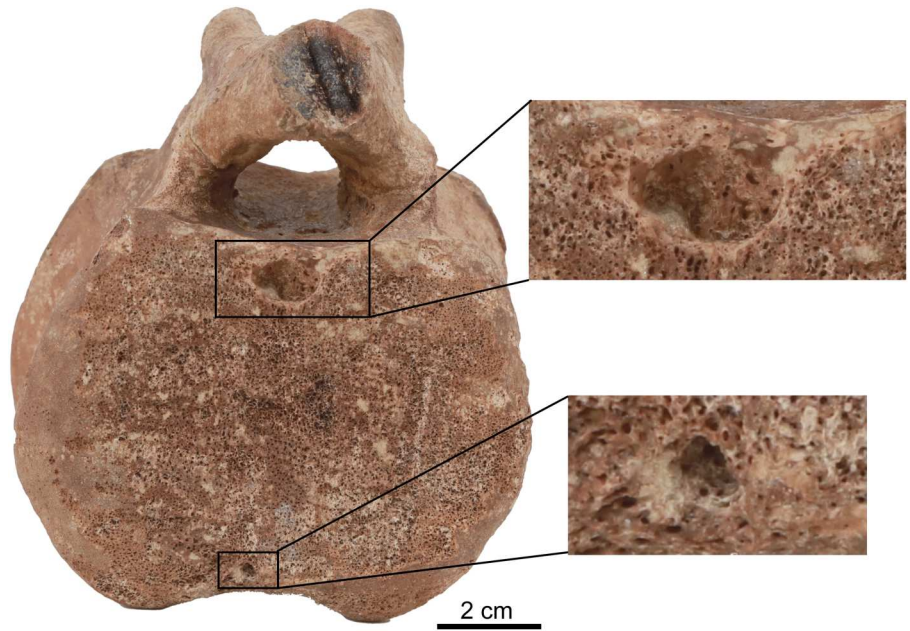


FIGURE 3. Distal caudal vertebrae HRS14005 from *Edmontosaurus annectens* with pseudopathologies. Vertebra shows postmortem textural changes on distal joint surface and depressions (close-up view).

exposure (Behrensmeyer, 1978; Egeland & Pickering, 2021). The shallow cortex deterioration appeared mostly on the inferior margin of rib fragment HRS02038, where the reactive bone is also present. However, on the unfractured distal end of the rib, similar cortex deterioration is also observed. We suggest that the “fine pitting” appearance in the cortex bone is most likely a result of postmortem regional bone exposure causing the delamination of cortical bone and giving the appearance of “fine pitting” due to the exposure of the medullary bone, especially in areas where the cortex is thinner, such as in the cortical surface associated with remodeling. However, this suggestion does not rule out the possibility of the presence of other bone diseases causing cortex bone porosity.

In our analysis, several other instances of pseudopathologies in bones are ultimately attributable to surface exposure causing diagenetic modifications to bone surface and damage to cortical bone (Table S1; Figs. 2 and 3). The linear grooves on metatarsal HRS12360 (Fig. 2B, C), were provisionally attributed to tooth traces upon first examination. These prominent parallel features could be classified as tooth traces based in the literature with descriptions for tooth traces (Binford, 1981; Jacobsen & Bromley, 2009; Mikuláš et al., 2006; Njau & Blumenschine, 2006; Pobiner, 2008; Pobiner et al., 2007). However, several other metatarsals in the assemblage also had grooves with similar orientation and location as the ones observed in HRS12360 (specimens HRS05166, HRS05420, HRS07530, HRS09092, HRS09784, HRS17323, HRS23162, HRS30652, available images in the SWAU fossil catalog database). Given the physical postmortem alteration, and the frequency of these cracks in metatarsals with similar orientation and location, we suggest that these features are most likely due to cracking displaying planes of cleavage associated with weaker areas in the bone, or parallel to the orientation of the primary fabric direction, at different stages of surface exposure to the environment (Behrensmeyer, 1978; Bishop et al., 2017; Pokines & Spiegel, 2021; Symes et al., 2014). To further confirm this suggestion, histological analysis would be beneficial in future study.

The surface of the cervical vertebra HRS10676 (Fig. 2A) displays several destructive depressions, indicating the deterioration of the cortical bone. Flaking and cracking on the cortical

surface is also observed. No bone reaction is displayed in the margins and surface of these depressions that erode from cortex into the medullary bone. Surface bone changes like that described in bone HRS10676 have been previously suggested to be a result of bone surface exposure to environmental factors (Behrensmeyer, 1978; Egeland & Pickering, 2020; Evans, 2021). However, there are some lytic bone diseases where bone reaction might not be present such as in acute infections destroying bone near time of death not giving enough time for bone response. It is also important to note that certain fungal diseases and bone reaction might also not be noticeable (Arkun, 2004; Hershkovitz et al., 1998). Several lesions in the surfaces of bone HRS10676, if pathological, are large enough to conclude that some time passed between time of the lesion and death. In this case, one would expect, based on size of the largest lesions, evidence of bone reaction. Thus, based on the collection of destructive depressions distributed throughout the bone surface, size of lesions accompanied by cracking and flaking, we suggest that the surface modification to HRS10676 is most likely a result of surface exposure to the environment before burial. However, it does not eliminate the possibility of a few pre-mortem lesions caused by an acute disease, near time of death. Histological analysis could be helpful to conclude the presence of a disease if some bone reaction was present in a microscopic scale.

#### Insect Boring Mimicking Lytic Lesions

An important subcategory of pseudopathology has turned out to be insect mediated bioerosion. Postmortem biogenetic erosion during surface exposure can mimic the lytic bone features of infectious, inflammatory, and degenerative bone diseases, which also erode bone via biogenetic routes. In lytic bone diseases, bone displacement occurs because of resorption caused by tumors, bacterial infections, or fungal diseases. In most of these cases, the eroded area is surrounded by a periosteal reaction, smooth eroded surfaces and margins (Hershkovitz et al., 1998). However, in fungal diseases the bone reaction is usually fine and frequently not present (Arkun, 2004; Hershkovitz et al., 1998). Thus, erosive depressions from surface exposure might



FIGURE 4. *Edmontosaurus annectens* ischium HRS12443 with modified surface texture. **A**, surface texture with shallow depressions suggestive of insect borings; **B**, closer view of bone surface with several individual elliptical shallow depressions and overlapping shallow depressions. Flaking of the cortical bone is also observed. Black arrows point to representative pits with scalloped edges and central pedestal.

be mistaken for a pathological lesion if not carefully examined for evidence of bone reactivity in association with other taphonomic processes.

Although the surface of bones within this collection are generally well-preserved enough to indicate rapid covering of bones during fossilization, signs of what appears to be attributable to biogenetic alterations is also suggested based on comparisons with previous work (Bader, 2008; Bader et al., 2009; Britt et al., 2008; Hasiotis et al., 1999; Odes et al., 2017; Pirrone et al., 2014a). Herein, we applied the comprehensive review of bone modifications interpreted to be produced by pupation chambers produced by insect larvae in Bader (2008) and Bader et al. (2009). The size, morphology, and distribution of pits in bone modifications reported are comparable to the modifications displayed in our study in the caudal vertebra HRS14005 and ischium HRS12443. The shallow pits and rosettes are generally described by circular to elliptical clusters of individual or overlapping shallow pits, averaging in general from 0.5–8 mm in diameter and <1 mm in depth (Bader, 2008; Bader et al., 2009) and are very similar to the ones found in the ischium

HRS12443. Especially in rosettes, the edges are scalloped, and some have an unmodified pedestal in the center of the pit just as observed in some of the examples found in HRS12443 (Fig. 4B). These are suggested to represent different stages of pupation when there might be presence of dry flesh and contact with the bone surface based on comparisons with modern examples (Bader, 2008; Bader et al., 2009; Serrano-Brañas et al., 2018). It is important to note that the ischium HRS12443 also displays other diagenetic modifications on the bone surface such as flaking, caused by the further degradation of cortical bone suggesting surface exposure to the environment. Given the real-world constraints of rare specimen preservation, this ischium was not sectioned; although sectioning would have resolved any diagnostic ambiguity, its bone tissue was readily observable on the surface and similar to other cited specimens.

In the same study by Bader (2008) and Bader et al. (2009), other depressions are described as hemispherical pits. These presented no overlapping occurrences, smooth walls with no scalloped edges, ranging from 1.98–5.63 mm in diameter and 0.62–1.74 mm in depth. These are interpreted as surface bone

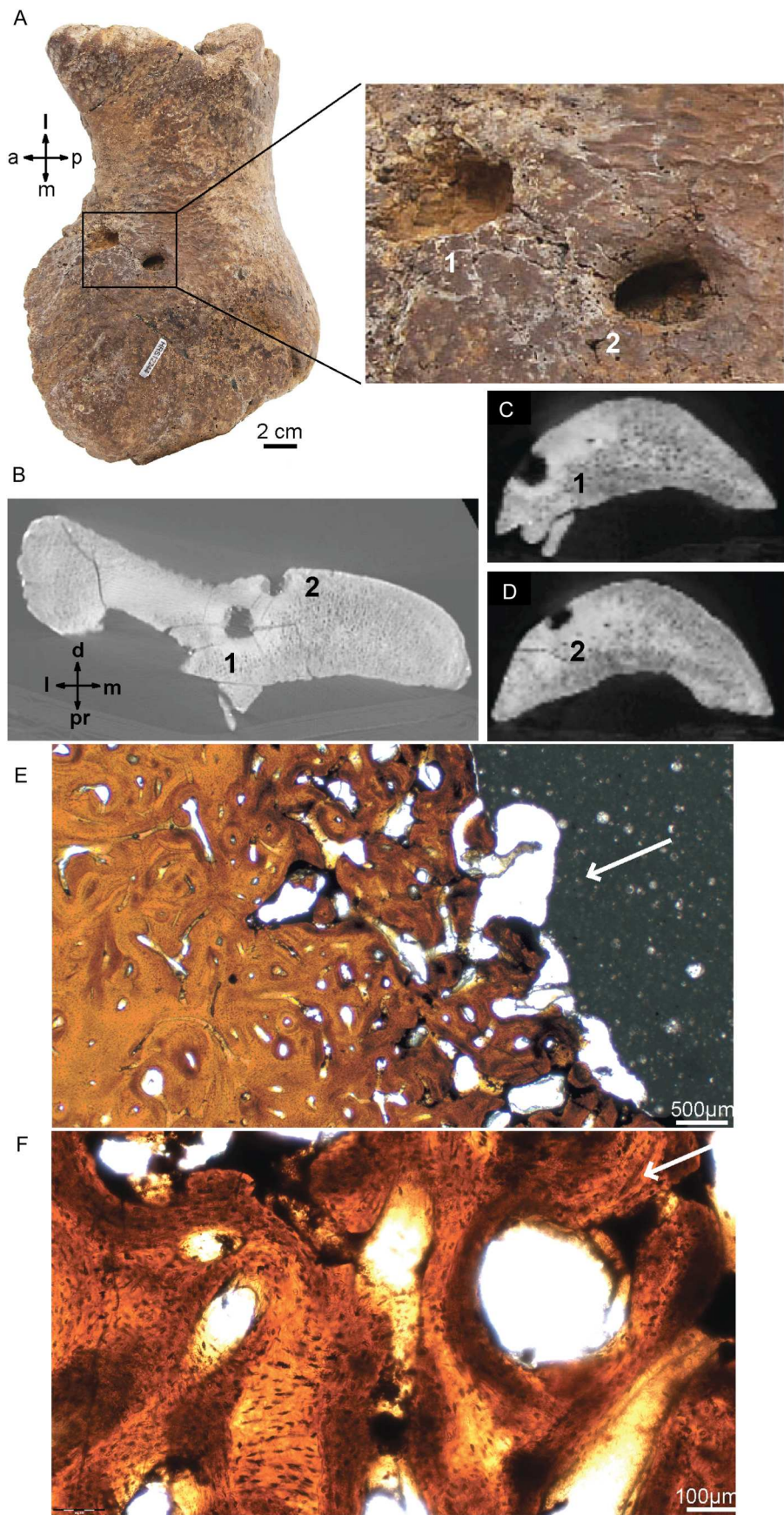


FIGURE 5. Right astragalus HRS12244 from *Edmontosaurus annectens* with depressions indicative of insect boring. **A**, orientation and closer view of the specimen and depressions (with numbering identification); **B**, sagittal view of CT scan imaging of depressions showing brighter regions near depressions; **C**, coronal view of depression identified as 1; **D**, coronal view of depression identified as 2; **E**, histological view (at 2 $\times$ ) of the surface area of the depression, with more hematite concentrations indicated by the darker red regions near the surface; **F**, closer view (at 10 $\times$ ) of the surface area of depression 1. White arrow points away from depression into the bone. **Abbreviations:** **a**, anterior; **d**, distal; **l**, lateral; **m**, medial; **p**, posterior; **pr**, proximal.

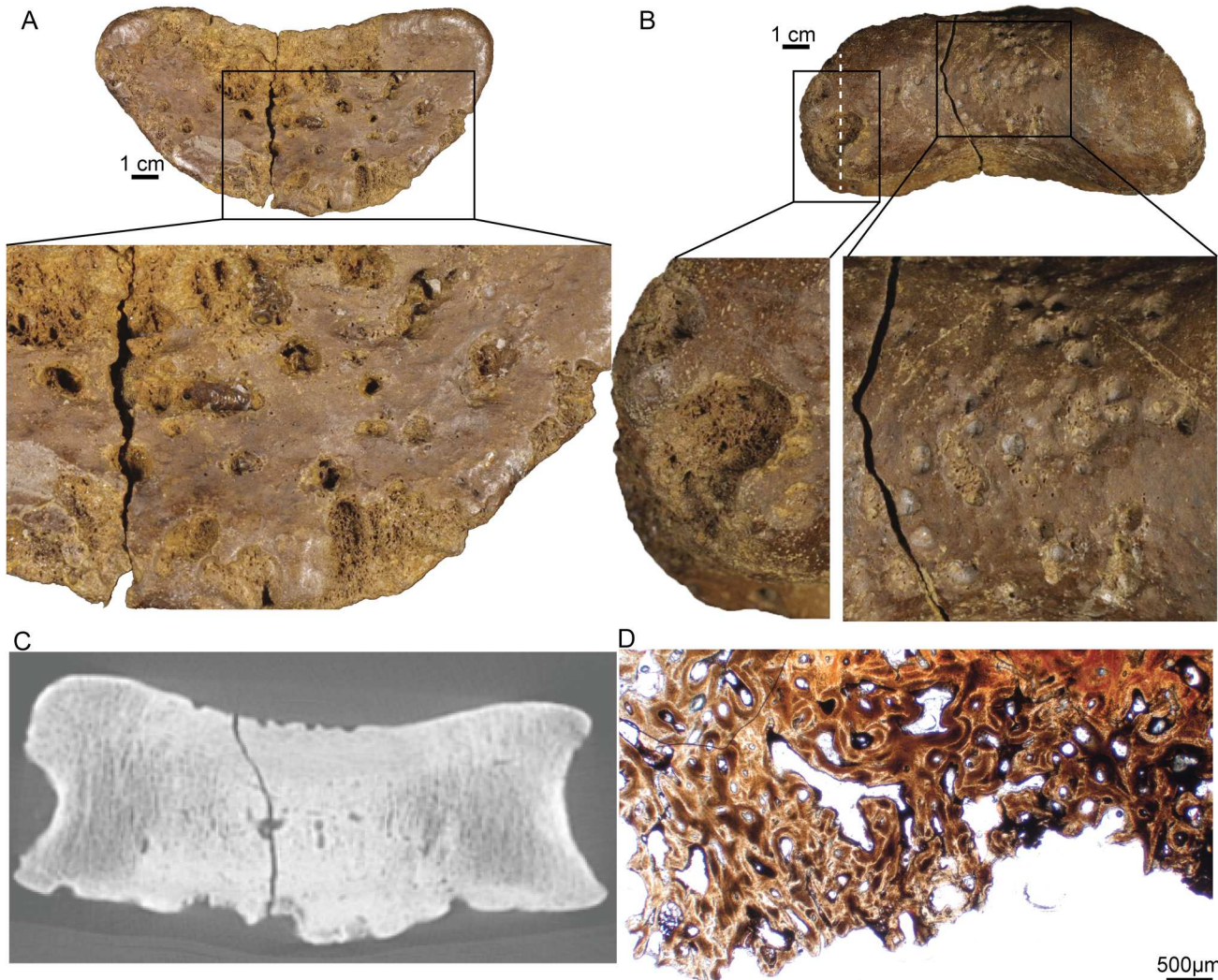


FIGURE 6. Pedal phalanx III-2 HRS09967 from *Edmontosaurus annectens* with insect borings. **A**, view of proximal articular surface with depressions with selected region for a close-up view of depressions; **B**, view of distal articular surface with depressions with selected regions for a close-up view of depressions; **C**, CT scan imaging indicating no particular bone reaction associated with depressions; **D**, histological image (in 2 $\times$ ) of the surface depth (associated the dashed white line in 6B) showing lamellar bone and postmortem erosive surface.

modifications caused by pupation chambers formed by insect larvae almost entirely within the bone. This interpretation is based on morphological similarities of these trace fossils to modern, bone-altering dermestid beetles for example (Bader, 2008; Bader et al., 2009). Such bone modifications with similar features are also displayed in two specific depressions in the caudal surface of the vertebra HRS14005 (Fig. 3). Thus, we suggest that these two hemispherical pits are also possibly a result of bioerosion. It is important to note that on the distal and proximal intervertebral articular surfaces of the HRS14005 centrum, the small shallow regular depressions/pits displayed throughout the surface, most likely indicate the deterioration of cortical bone exposing the medullary bone. This feature is also observed on the previously discussed rib fragment HRS02038 (Fig. 1B, C) suggesting diagenetic modifications due to bone exposure to the environment.

The depressions observed in the distal articular surface of the pedal phalanx HRS09967 are similar to the previously described depressions as a result of postmortem bioerosion of elliptical to round depressions with diameters ranging from 1–5 mm and 1 mm in depth not penetrating the trabecular bone (Britt et al., 2008; Hasiotis et al., 1999). Likewise, similar depressions as the

ones found in the proximal articular surface of HRS09967 (and a few in the edge of distal articular surface), have been described and classified as holes that can occur individually or grouped. The depth of these holes penetrates the trabecular bone (Odes et al., 2017; Pirrone et al., 2014a).

Although they may vary in morphology, depth, and patterns, the depressions observed in the caudal vertebra HRS14005, ischium HRS12443, and pedal phalanx HRS09967 most likely indicate postmortem alterations to the bones caused by insect or larvae boring. These alterations, due to exposure, have also been associated with diagenetic processes (HRS14005 and HRS09967) including flaking (HRS12443) (Behrensmeyer, 1978; Egeland & Pickering, 2021; Evans, 2021). Thus, the combination of abrasion and bioerosion on the surface of these bones most likely suggests diagenetic and biogenetic alterations due to exposure of remains.

The astragalus HRS12244 depressions (Fig. 5) may superficially resemble punctures made by a tooth with a semicircular cross section. Given the blunt roundness of the depression at its nadir, the only tooth aligned with the associated fauna able to produce such marks would be a worn crocodilian tooth. However, the shape of the depression is a poor match even

with this scenario, given the depressions have both a smaller neck on the surface and no preserved tooth shape at depth. However, one should still observe internally the outline of a tooth shape in its entire depth. **Figure 5B, C, and D** show that at mid-depth, the diameter of the depression is larger than its inner-most depth and even smaller at the surface opening. The lesions in the HRS12244 are comparable with other previously reported examples, specifically reported as a result of bioerosion by necrophagous larvae of a terrestrial arthropod (Lima, 2017; Odes et al., 2017; Pirrone et al., 2014a; Pirrone et al., 2014b; Zanetti et al., 2019).

CT scanning supported the initial impression of the poor fit of the shape of the depression to a tooth puncture wound. However, the intensely radiopaque area (**Fig. 5A, B, C, D**) manifest resembled the sclerotic bone indicating pre-mortem bone reaction seen on images from live individuals. Sclerotic bone formation is a well-documented chronic response of bone to trauma and infection in the radiological literature of humans and other vertebrates. Following this interpretation, the bright outline surrounding the depressions could indicate healing from a pre-mortem lesion. However, a critical distinction in comparing fossil bones with medical and veterinary literature is also recognizing the role that depositional environments may play in creating bone changes. SEM-EDS analysis indicates higher density of iron and sulfur adjacent to the reported lesions. It has been reported that during microorganism invasion of tissues, iron is sequestered from the blood, which is crucial for their proliferation within the host's tissue (Bullen, 1981; Cornelissen & Sparling, 1994). Therefore, an increase in iron near the affected area may occur as iron is being captured and transported into the parasite. However, histological analysis of our specimen HRS12244 shows hematite ( $Fe_2O_3$ ) crystals in higher density adjacent to the reported lesions (**Fig. S2**), thus supporting the results from SEM-EDS elemental analysis. Hematite precipitation may be from recent weathering of pyrite that is more widely distributed in the bone. These findings have been previously reported in fossils from the Lance Formation (Sawlowicz & Kaye, 2006). Another option for the presence of hematite is that it could have been added with infiltrated clays during burial (note clay minerals filling the depression in **Fig. S2**). The CT scans show intense radiopacity in the region adjacent to the lesions. The microscopic examinations indicating the mineralogy adjacent to lesion suggest that mineralization increased the bone density, thus producing the halo adjacent to the lesion in the CT scan image. Mineral replacement from a less dense to a denser composition can also create brighter radiographic images. Hematite has an attenuation coefficient almost 4× greater than apatite (Bam et al., 2020). These changes are not associated with bone remodeling but resulted from diagenetic changes, with precipitation of minerals adjacent to the lesions. This finding is consistent with the histological presentation of fibrolamellar bone architecture in the section with no response at the truncated layers adjoining these lesions (**Fig. 5E, F**). Thus, we conclude that the overwhelming evidence points to the main factor causing the bone alteration of the astragalus HRS12244 (shape of depression, histological features, mineral precipitation, and replacement) is attributable to postmortem manifestations of pupal chambers resulting from boring larvae, not bone response to infection. The observable, more highly vascularized and presumably actively growing bone extends beyond the area delimited by the depression and is associated with the cortical adjacent areas of a weight-bearing articular surface.

## CONCLUSION

Manifestations of pseudopathologies in the fossil bones often result from biogenetic and diagenetic taphonomic processes.

Since they are postmortem modifications to bones, interpretations of their causes can yield postmortem environmental conditions and settings associated with bones. Thus, the correct characterization and distinction of bone abnormalities such as paleopathologies or pseudopathologies are crucial to analyses of disease.

In our analysis of bone abnormalities from a monospecific *Edmontosaurus annectens* bone bed collection, we encountered several manifestations of pseudopathologies caused by postmortem modifications. We conclude that the different types of pseudopathologies are indicative of the postmortem and pre-burial processes. Moreover, in the astragalus specimen, without the ground truth of the histology, an erroneous interpretation of the CT radiopacity might have transpired. SEM-EDS analysis suggests diagenetic changes associated with the corresponding region of the radiopacity shown in the CT scan. Histology reveals the lack of reactive bone and supports the interpretation of these depressions as bioerosion resulting from terrestrial arthropods boring on the bones during larval stages and forming pupal chambers. Burrow sizes, morphologies, and arrangement represent different insects of different sizes and infestations. Due to analogs of insect burrows on carcasses and their association with the environment (Britt et al., 2008; Martin & West, 1995; West & Martin, 2002), we conclude that the carcasses of the *E. annectens* population represented within the bonebed, were partially covered by flesh and exposed subaerially for some time prior to burial. All bones reported were excavated and not subject to modern weathering due to surface exposure. Pre-burial exposure of remains is also suggested by the occasional manifestations of erosive or abrasive postmortem pitting/depressions on bones, indicating weathering. However, since within the bonebed the majority of the bones are well-preserved, disarticulated, and dissociated, we conclude that the carcasses were exposed for just enough time for decomposition, occasional bioerosion, and disarticulation. The frequency of the early postmortem distal end rib fractures suggests scavenging, thus supporting our conclusion that the carcasses were exposed for some time (sufficient time for scavenging). Tooth trace manifestations in various bone types (Siviero et al., 2020b) also support scavenging. However, early postmortem transport can also account for some of the rib fractures.

Following exposure, due to the bonebed depositional setting, the remains from this *E. annectens* population were transported and buried in a mass flow event as previously suggested (Snyder et al., 2020; Weeks, 2016).

Our observations on several specimens correspond to the taphonomic traces of insects as described in the literature. We similarly “diagnose” such traces in this sample as insect borings or pupal chambers from necrophagous larvae, suggesting infestation of exposed carcasses. Additionally, perimortem fractures are frequently observed on ribs, particularly on their distal end, suggesting postmortem ribcage trauma incurred during scavenging. Manifestations of tooth traces in other bones also suggest scavenging. Other erosive pseudopathologies indicate postmortem weathering, thus strengthening our conclusions of a period of carcass exposure before burial. However, the uniformly good surface preservation of most bones within the bed further indicates that this period of exposure on the ground was likely not protracted.

In future work, the continued study of bone abnormalities suggestive of biogenetic and diagenetic taphonomic processes (pseudopathologies) is important to (1) add to this research data analysis, (2) strengthen our conclusions on the taphonomic setting associated with the animals within this bonebed, (3) add to the literature pertaining to pseudopathologies providing a cautionary tale that CT image alone might not be sufficient

depending on the lesion. Where possible, histological thin sections can be beneficial for diagnosis.

## ACKNOWLEDGMENTS

We thank the HRS owners for granting land access associated with the bonebed of this study. We also thank all the volunteers for their efforts in excavating and preparing the bones. SWAU for granting access and assistance to the fossil collection, D. Kido at LLMC for assisting with CT scanning of bones, and L. Brand at LLU for academic assistance during this project. We also thank R. Chase, L. Denhan, and K. Wright at LLU for histological remarks, J. McLarty for assistance with images (specimens HRS10676 and HRS14005), B. Rothschild for his comments to this manuscript, and editor and reviewers for their suggestions to improve this manuscript. Funding to this research was provided by LLU.

## AUTHOR CONTRIBUTIONS

BCTS designed the project, selected material to be analyzed, analyzed the data, and drafted the manuscript including the images and supplementary files. ER also helped to design the project and analyze the data. KEN helped to analyze the data. AVC gathered the material. All authors edited the manuscript.

## DATA AVAILABILITY STATEMENT

The data necessary to reproduce the results of the manuscript are available at: <https://fossil.swau.edu> for fossil catalog; and MorphoSource <https://www.morphosource.org> for the CT images and raw files for the thin sections from HRS12244 (search as 12244) and HRS09967 (search as 9967).

## DISCLOSURE STATEMENT

No potential conflict of interest was reported by the author(s).

## ORCID

Bethania C. T. Siviero  <http://orcid.org/0009-0009-8456-0227>  
 Elizabeth Rega  <http://orcid.org/0009-1128-7020>  
 Kevin E. Nick  <http://orcid.org/0000-0002-8476-1127>  
 Art V. Chadwick  <http://orcid.org/0000-0003-4133-160X>

## SUPPLEMENTARY FILE

Supplementary File .docx: Additional supporting information. Figure S1, ribs with postmortem fractures of distal ends. Figure S2, Histological analysis of astragalus HRS12244 with SEM/EDS and compound microscope. Table S1, Description of bone surface modification examples from a monospecific *Edmontosaurus annectens* bonebed from the Lance Formation (WY).

## LITERATURE CITED

Arkun, R. (2004). Parasitic and fungal disease of bones and joints. *Seminars in musculoskeletal radiology*, 8(3), 231–242. doi:10.1055/s-2004-835363

Bader, K. S. (2008). *Insect trace fossils on dinosaur bones from the Upper Jurassic Morrison Formation, northeastern Wyoming, and their use in vertebrate taphonomy* [Master's thesis, University of Kansas]. University of Kansas ScholarWorks Archive. University of Kansas.

Bader, K. S., Hasiotis, S. T., & Martin, L. D. (2009). Application of forensic science techniques to trace fossils on dinosaur bones from a quarry in the Upper Jurassic Morrison Formation, northeastern Wyoming. *Palaios*, 24(3), 140–158. doi:10.2110/palo.2008.p08-058

Bam, L. C., Miller, J. A., & Becker, M. (2020). A mineral X-ray linear attenuation coefficient tool (MXLAC) to assess mineralogical differentiation for X-ray computed tomography scanning. *Minerals*, 10(5), 441. doi:10.3390/min10050441

Behrensmeyer, A. K. (1978). Taphonomic and ecologic information from bone weathering. *Paleobiology*, 4(2), 150–162. doi:10.1017/S0094837300005820

Binford, L. R. (1981). From Patterns of bone modifications produced by nonhuman agents, *Bones: Ancient Men and Modern Myths* (pp. 35–86). Academic Press.

Bishop, P. J., Clemente, C. J., Hocknull, S. A., Barrett, R. S., & Lloyd, D. G. (2017). The effects of cracks on the quantification of the cancellous bone fabric tensor in fossil and archaeological specimens: a simulation study. *Journal of Anatomy*, 230(3), 461–470. doi:10.111/joa.12569

Blau, S. (2017). The effects of weathering on bone preservation. In E. M. J. Schotsmans, N. Márquez-Grant, & S. L. Forbes (Eds.), *Taphonomy of Human Remains: Forensic Analysis of the Dead and the Depositional Environment: Forensic Analysis of the Dead and the Depositional Environment* (pp. 201–211). Wiley.

Britt, B. B., Scheetz, R. D., & Dangerfield, A. (2008). A Suite of dermestid beetle traces on dinosaur bone from the Upper Jurassic Morrison Formation, Wyoming, USA. *Ichnos*, 15(2), 59–71. doi:10.1080/10420940701193284

Bullen, J. J. (1981). The significance of iron in infection. *Clinical Infectious Diseases*, 3(6), 1127–1138. doi:10.1093/clinids/3.6.1127

Chinsamy, A., Thomas, D. B., Tumarkin-Deratzian, A. R., & Fiorillo, A. R. (2012). Hadrosaurs were perennial polar residents. *The Anatomical Record*, 295(4), 610–614. doi:10.1002/ar.22428

Conard, N. J., Walker, S. J., & Kandel, A. W. (2008). How heating and cooling and wetting and drying can destroy dense faunal elements and lead to differential preservation. *Palaeogeography, Palaeoclimatology, Palaeoecology*, 266(3-4), 236–245. doi:10.1016/j.palaeo.2008.03.036

Cornelissen, C. N., & Sparling, P. F. (1994). Iron piracy: acquisition of transferrin-bound iron by bacterial pathogens. *Molecular microbiology*, 14(5), 843–850. doi:10.1111/j.1365-2958.1994.tb01320.x

Corron, L., Huchet, J. B., Santos, F., & Dutour, O. (2017). Using classifications to identify pathological and taphonomic modifications on ancient bones: Do “taphonomic” criteria exist? *Bulletins et Mémoires de la Société d’Anthropologie de Paris*, 29(1–2), 1–18.

Csiki, Z. (2006). Insect borings in dinosaur bones from the Maastrichtian of the Hațeg Basin, Romania—paleoecological and paleoclimatic implications. *Mesozoic and Cenozoic Vertebrates and Paleoenvironments. Tributes to the career of Dan Grigorescu, Ed. Ars Docendi*, 95–104.

Egeland, C. P., & Pickering, T. R. (2021). Cruel traces: Bone surface modifications and their relevance to forensic science. *Wiley Interdisciplinary Reviews: Forensic Science*, 3(3), e1400.

Evans, T. (2021). Fluvial taphonomy. In J. T. Pokines, E. N. L'Abbé, & S. A. Symes (Eds.), *Manual of forensic taphonomy* (pp. 163–192). CRC Press.

Hackett, C. J. (1981). Microscopical focal destruction (tunnels) in exhumed human bones. *Medicine, Science and the Law*, 21(4), 243–265. doi:10.1177/002580248102100403

Halstead, L. B. (1990). Palaeopathology. In D. E. Briggs, & P. R. Crowther (Eds.), *Palaeobiology: A synthesis* (pp. 381–385). Blackwell Science.

Hanna, R. R. (2002). Multiple injury and infection in a sub-adult theropod dinosaur *Allosaurus fragilis* with comparisons to allosaur pathology in the Cleveland-Lloyd Dinosaur Quarry Collection. *Journal of Vertebrate Paleontology*, 22(1), 76–90. doi:10.1671/0272-4634(2002)022[0076:MAIAIA]2.0.CO;2

Hasiotis, S. T., Fiorillo, A. R., Hanna, R. R., & Gillette, D. D. (1999). Preliminary report on borings in Jurassic dinosaur bones: Evidence for invertebrate-vertebrate interactions. *Vertebrate Paleontology in Utah. Utah Geological Survey Miscellaneous Publication*, 99(1), 193–200.

Hershkovitz, I., Rothschild, B. M., Dutour, O., & Greenwald, C. (1998). Clues to recognition of fungal origin of lytic skeletal lesions. *American Journal of Physical Anthropology*, 106(1), 47–60. doi:10.1002/(SICI)1096-8644(199805)106:1<47::AID-AJPA4>3.0.CO;2-A

Holland, T. D., & O'Brien, M. J. (1997). Parasites, porotic hyperostosis, and the implications of changing perspectives. *American Antiquity*, 62(2), 183–193. doi:10.2307/282505

Jacobsen, A. R., & Bromley, R. G. (2009). New ichnotaxa based on tooth impressions on dinosaur and whale bones. *Geological Quarterly*, 53, 373–382.

Johnson, V., Beckett, S., & Márquez-Grant, N. (2017). Differentiating human versus non-human bone by exploring the nutrient foramen: implications for forensic anthropology. *International journal of legal medicine*, 131(6), 1757–1763. doi:10.1007/s00414-017-1662-y

Kizilkiranat, E., Boyan, N., Ozsahin, E. T., Soames, R., & Oguz, O. (2007). Location, number and clinical significance of nutrient foramina in human long bones. *Annals of Anatomy - Anatomischer Anzeiger*, 189(1), 87–95. doi:10.1016/j.anamat.2006.07.004

Landry, P. S., Marino, A. A., Sadasivan, K. K., & Albright, J. A. (2000). Effect of soft-tissue trauma on the early periosteal response of bone to injury. *The Journal of Trauma: Injury, Infection, and Critical Care*, 48(3), 479–483. doi:10.1097/00005373-200003000-00018

Lima, F. C. G. D. (2017). Alterações ante mortem e pseudopatologias em exoesqueleto de cingulados pleistocénicos de grande porte da região intertropical brasileira [Master's thesis, Universidade Federal Rural do Semi-Árido]. Universidade Federal Rural do Semi-Árido Theses and Dissertation Archives.

Lin, J. T., & Lane, J. M. (2004). Osteoporosis. *Clinical Orthopaedics and Related Research*, 425, 126–134. doi:10.1097/01.blo.0000132404.30139.f2

Littleton, J. (2000). Taphonomic effects of erosion on deliberately buried bodies. *Journal of Archaeological Science*, 27(1), 5–18. doi:10.1006/jasc.1999.0436

Lopes, R. P., & Ferigolo, J. (2015). Post mortem modifications (pseudopathologies) in middle-late Pleistocene mammal fossils from southern Brazil. *Revista brasileira de paleontologia*, 18(2), 285–306. doi:10.4072/rbp.2015.2.09

Mann, R. W., & Hunt, D. R. (2013). *Photographic regional atlas of bone disease: a guide to pathologic and normal variation in the human skeleton* (3<sup>rd</sup> ed.). Charles C Thomas Publisher.

Martin, L. D., & West, D. L. (1995). The recognition and use of dermestid (Insecta, Coleoptera) pupation chambers in paleoecology. *Palaeogeography, Palaeoclimatology, Palaeoecology*, 113(2-4), 303–310. doi:10.1016/0031-0182(95)00058-T

Martin, M. (2008). Paleopathological Methodology: Macroscopic Analysis Fails to Make the Grade. *The University of Western Ontario Journal of Anthropology*, 16(1).

Mikuláš, R., Kadlecová, E., Fejfar, O., & Dvořák, Z. (2006). Three new ichnogenera of biting and gnawing traces on reptilian and mammalian bones: a case study from the Miocene of the Czech Republic. *Ichnos*, 13(3), 113–127. doi:10.1080/10420940600850729

Njau, J. K., & Blumenschine, R. J. (2006). A diagnosis of crocodile feeding traces on larger mammal bone, with fossil examples from the Plio-Pleistocene Olduvai Basin, Tanzania. *Journal of Human Evolution*, 50(2), 142–162. doi:10.1016/j.jhevol.2005.08.008

Odes, E. J., Parkinson, A. H., Randolph-Quinney, P. S., Zipfel, B., Jakarta, K., Bonney, H., & Berger, L. R. (2017). Osteopathology and insect traces in the *Australopithecus africanus* skeleton StW 431. *South African Journal of Science*, 113(1/2), 7–7. doi:10.17159/sajs.2017/20160143

Petersen, K., Isakson, J. I., & Madsen Jr, J. H. (1972). Preliminary study of paleopathologies in the Cleveland-Lloyd dinosaur collection. *Utah Academy Proceedings*, 49(1), 4447.

Pirrone, C. A., Buatois, L. A., & Bromley, R. G. (2014a). Ichnotaxobases for bioerosion trace fossils in bones. *Journal of Paleontology*, 88(1), 195–203. doi:10.1666/11-058

Pirrone, C. A., Buatois, L. A., & González Riga, B. (2014b). A new ichnospecies of *Cubiculum* from Upper Cretaceous dinosaur bones in Western Argentina. *Ichnos*, 21(4), 251–260. doi:10.1080/10420940.2014.958225

Pobiner, B. (2008). Paleoecological information in predator tooth marks. *Journal of Taphonomy*, 6(3), 373–397.

Pobiner, B. L., DeSilva, J., Sanders, W. J., & Mitani, J. C. (2007). Taphonomic analysis of skeletal remains from chimpanzee hunts at Ngogo, Kibale National Park, Uganda. *Journal of human evolution*, 52(6), 614–636. doi:10.1016/j.jhevol.2006.11.007

Pokines, J. T., & Higgs, N. D. (2021). Marine environmental alterations to bone. In J. T. Pokines, E. N. L'Abbé, & S. A. Symes (Eds.), *Manual of forensic taphonomy* (pp. 193–250). CRC Press.

Pokines, J. T., & Spiegel, C. (2021). Subaerial weathering and other terrestrial surface taphonomic processes. In J. T. Pokines, E. N. L'Abbé, & S. A. Symes (Eds.), *Manual of Forensic Taphonomy* (pp. 403–442). CRC Press.

Resnick, D. (1995). Physical injury: concepts and terminology. *Diagnosis of bone and joint disorders* (pp. 2561–2692). Saunders.

Rixford, E. (1913). On the mechanics of production of certain fractures. *Journal of the American Medical Association*, 61(12), 916–920. doi:10.1001/jama.1913.04350120006002

Roberts, E. M., Rogers, R. R., & Foreman, B. Z. (2007). Continental insect borings in dinosaur bone: examples from the Late Cretaceous of Madagascar and Utah. *Journal of Paleontology*, 81(1), 201–208. doi:10.1666/0022-3360(2007)81[201:CIBIDB]2.0.CO;2

Rothschild, B. M., Surmik, D., & Bertozzo, F. (2023). *Modern Paleopathology, the Study of Diagnostic Approach to Ancient Diseases, their Pathology and Epidemiology: Let there Be Light, the Light of Science and Critical Thinking*. Springer.

Sawlowicz, Z., & Kaye, T. G. (2006). Replacement of iron sulphides by oxides in the dinosaur bone from the Lance Fm. (Wyoming, USA)—preliminary study. *Mineralogia Polonica Special Papers*, 29, 184–187.

Schultz, J. J., & Dupras, T. L. (2021). Identifying the origin of taphonomic bone staining and color changes in forensic contexts. In J. T. Pokinwa, E. N. L'Abbé, & S. A. Symes (Eds.), *Manual of forensic taphonomy* (pp. 443–472). CRC Press.

Scott, E., Rega, E., Scott, K., Bennett, B., & Sumida, S. (2015). A pathological timber wolf (*Canis lupus*) femur from Rancho La Brea indicates extended survival after traumatic amputation injury. *Natural History Museum of Los Angeles County Science Series*, 42, 33–36.

Seeman, E. (2013). Age- and menopause-related bone loss compromise cortical and trabecular microstructure. *The Journals of Gerontology Series A: Biological Sciences and Medical Sciences*, 68(10), 1218–1225. doi:10.1093/gerona/glt071

Seymour, R. S., Caldwell, H. R., Woodward, H. N., & Hu, Q. (2024). Growth rate affects blood flow rate to the tibia of the dinosaur *Mayasaura*. *Paleobiology*, 50(1), 123–129. doi:10.1017/pab.2023.24

Serrano-Brañas, C. I., Espinosa-Chávez, B., & Maccracken, S. A. (2018). Insect damage in dinosaur bones from the Cerro del Pueblo Formation (Late Cretaceous, Campanian) Coahuila, Mexico. *Journal of South American Earth Sciences*, 86, 353–365. doi:10.1016/j.jsames.2018.07.002

Sharma, A. K., Toussaint, N. D., Masterson, R., Holt, S. G., Rajapakse, C. S., Ebeling, P. R., Mohanty, S. T., Baldock, P., & Elder, G. J. (2018). Deterioration of cortical bone microarchitecture: critical component of renal osteodystrophy evaluation. *American Journal of Nephrology*, 47(6), 376–384. doi:10.1159/000489671

Siviero, B. C. T. (2019). *Behavioral Causes of Paleopathologies in Cretaceous Edmontosaurus annectens, Lance Formation, Wyoming* [Doctoral dissertation, Loma Linda University]. Loma Linda University ProQuest Theses and Dissertations Archive.

Siviero, B. C. T., McLain, M. A., Nelsen, D., Brand, L. R., & Chadwick, A. V. (2017, October 22–25). *Refinement of tooth trace criteria through experimentation and literature review* [Poster presentation]. Geological Society of America Annual Meeting, Seattle, WA, United States of America.

Siviero, B. C. T., Rega, E., Hayes, W. K., Cooper, A. M., Brand, L. R., & Chadwick, A. V. (2020a). Skeletal trauma with implications for intratail mobility in *Edmontosaurus annectens* from a monodominant bonebed, Lance Formation (Maastrichtian), Wyoming USA. *Palaios*, 35(4), 201–214. doi:10.2110/palo.2019.079

Siviero, B. C. T., Rega, E., McLain, M., Brand, L., Chadwick, A., & Nelsen, D. (2020b, October 11–17). *Identification of Tooth Traces from an Edmontosaurus annectens Bonebed within The Lance Formation (Maastrichtian), Wyoming*. [Poster presentation]. Society of Vertebrate Paleontology, 80th Annual Virtual Meeting.

Snyder, K., McLain, M., Wood, J., & Chadwick, A. (2020). Over 13,000 elements from a single bonebed help elucidate disarticulation and transport of an *Edmontosaurus thanatocoenosis*. *PLoS ONE* 15(5), Article E0233182 doi:10.1371/journal.pone.0233182

Stuart-Macadam, P. (1991). Porotic hyperostosis: changing interpretations. *Human paleopathology: Current syntheses and future options*, 87, 36–39.

Symes, S. A., L'Abbé, E. N., Stull, K. E., LaCroix, M., & Pokines, J. T. (2014). Taphonomy and the timing of bone fractures in trauma

analysis. In J. T. Pokinwa, E. N. L'Abbé, & S. A. Symes (Eds.), *Manual of forensic taphonomy* (pp. 341–365). CRC Press.

Thompson, C. E., Ball, S., Thompson, T. J., & Gowland, R. (2011). The abrasion of modern and archaeological bones by mobile sediments: the importance of transport modes. *Journal of Archaeological Science*, 38(4), 784–793. doi:10.1016/j.jas.2010.11.001

Weeks, S. R. (2016). *Depositional Model of a Late Cretaceous Dinosaur Fossil Concentration, Lance Formation* [Master's thesis, Loma Linda University]. Loma Linda University Theses and Dissertations Archive.

West, D. L., & Martin, L. D. (2002). Insect trace fossils as environmental/taphonomic indicators in archaeology and paleoecology. In *TER-QUA symposium series*, 3, 163–173.

Whitney, M. R., Otoo, B. K., Angielczyk, K. D., & Pierce, S. E. (2022). Fossil bone histology reveals ancient origins for rapid juvenile growth in tetrapods. *Communications Biology*, 5(1), 1280. doi:10.1038/s42003-022-04079-0

Whiteside, L. A., & Lesker, P. A. (1978). The effects of extraperiosteal and subperiosteal dissection. II. On fracture healing. *The Journal of Bone & Joint Surgery*, 60(1), 26–30. doi:10.2106/00004623-197860010-00004

Wiest, L. A., Ferraro, J. V., Binetti, K. M., Forman, S. L., Esker, D. A., Kibunja, M., Brugal, J. P., & Zechmann, B. (2018). Morphological characteristics of preparator air-scribe marks: Implications for taphonomic research. *PloS ONE*, 13(12), Article E0209330. doi:10.1371/journal.pone.0209330

Wolff, E. D., Salisbury, S. W., Horner, J. R., & Varricchio, D. J. (2009). Common avian infection plagued the tyrant dinosaurs. *PLoS One*, 4(9), e7288. doi:10.1371/journal.pone.0007288

Zanetti, N. I., Ferrero, A. A., & Centeno, N. D. (2019). Depressions of *Dermestes maculatus* (Coleoptera: Dermestidae) on bones could be pupation chambers. *American Journal of Forensic Medicine & Pathology*, 40(2), 122–124. doi:10.1097/PAF.0000000000000449

Zoetis, T., Tassinari, M. S., Bagi, C., Walther, K., & Hurt, M. E. (2003). Species comparison of postnatal bone growth and development. *Birth Defects Research Part B: Developmental and Reproductive Toxicology*, 68(2), 86–110. doi:10.1002/bdrb.10012

Handling Editor: Daniel Madzia.